Prospective Rigid-Body Motion Correction Using Miniature Wireless RF-Coils as Position Tracking Probes

Melvyn B. Ooi[1], Murat Aksoy[1], Julian Maclaren[1], Ronald D. Watkins[1], and Roland Bammer[1]
[1]*Radiology, Stanford University, Stanford, CA, United States*

Introduction: The use of miniature radio-frequency (RF) coils as position-tracking probes (1,2) has been the foundation of several advances in prospective motion correction (3-5). In recent works (6-8), subjects wore a headband containing three such RF coils, which tracked the head's orientation/position during brain MRI. We refer to these previously developed RF coils (1-8) as "*wired* markers", since each RF coil is connected to the scanner via a traditional electrical cable. While wired markers have been effectively employed in a research setting, their widespread adoption may be hampered by the wired connections between the headband and scanner.

We therefore present a novel RF coil based "*wireless* marker" approach for prospective motion correction of brain MRI, which is based on the principle of wireless inductive coupling between each wireless marker and the imaging head-coil. The elimination of any wired connection to the scanner provides several advantages: i) improved patient safety by removing the long, electrically conducting wires which are a potential source of RF heating and local SAR increase; ii) no additional RF receive channels are needed, since the tracking signal is detected via inductive coupling to the imaging head-coil; iii) ease-of-use, due to their small size and wire-free operation, thereby facilitating their portability to a high-throughput clinical setting. We demonstrate successful prospective correction in a moving phantom and head.

Theory & Methods: The underlying principle used for wireless-marker tracking is inductive signal coupling between two RF coils (i.e. Faraday's law of mutual induction). Even though two RF coils are not physically connected, a time-varying current in coil 1 (wireless marker) can induce an EMF in coil 2 (imaging head-coil) via the magnetic flux that links the two coils. During RF-receive, each wireless marker thus acts as a local signal amplifier that picks up the time-varying MR signal in its immediate vicinity; the signal is then inductively coupled to the nearby imaging head-coil, and thereby routed into the standard RF receiver. This concept has been used previously for wireless catheter visualization (9).

Experiments were performed on a 3T GE-MR750 scanner (WI, USA) using a standard 8-ch head-coil for imaging. Prospective correction is performed using three wireless markers in order to uniquely define any arbitrary rigid-body motion. Each wireless marker (Fig. 1a, left) is a miniature RF coil that is free of any mechanical connections to the scanner. It is a three-turn (dia ~ 4 mm) solenoid inductor and capacitor, tuned to the scanner resonant frequency (127.8 MHz). Inside the solenoid cavity is a silicone sphere (dia ~ 3 mm), which is the point-source that is tracked. Crossed diodes passively detune the resonant circuit during RF-transmit. Each wireless marker is encased in a self-contained capsule (Fig. 1a, middle). For phantom experiments, three capsules are rigidly attached to the phantom. For in vivo experiments, the volunteer wears a pair of glasses (Fig. 1b) that is designed and 3D-printed (Stratasys Fortus 360mc, MN, USA) with three wireless-marker capsules integrated into its frame.

Wireless-marker positions in 3D are measured using a tracking pulse-sequence (2,6) that consists of a non-selective RF-pulse ($\alpha = 5°$) and gradient-echo projections in three orthogonal xyz-directions (FOV = 300 mm, N = 256, duration = 15 ms). The sum-of-squares signal from the 8-ch head-coil after the x-projection (Fig. 1c) clearly shows the location of all three wireless markers along the physical x-axis of the scanner. The correspondence problem of determining which peak belongs to which wireless marker is resolved using *a priori* knowledge of the relative placement of each wireless marker. For example, each wireless-marker in the glasses is assigned a number (Fig. 1b). The peaks in the x-projection (Fig. 1c) will then be read out in the order of their appearance on the x-axis (right-to-left of Fig. 1b, see inset axes).

Prospective motion correction was applied to a 2D-GRE scan between every phase-encode by using the tracking pulse-sequence and a similar real-time scan-plane update mechanism as described in (6). For both a phantom and volunteer, two cases were tested: i) resting; ii) performing a series of reproducible, deliberate motions during the scan. For each case, two scans were acquired – with correction ON and OFF.

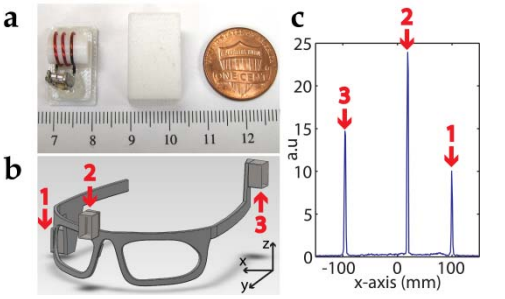

Fig. 1: *a) Wireless marker (left), enclosing capsule (middle), and U.S. penny (right) relative to ruler markings in mm. b) glasses integrated with 3 wireless markers for brain MRI. Red arrows denote locations of wireless markers, along with marker number c) Signal from 3 wireless markers after x-projection of tracking pulse-sequence, as received by the 8-ch head-coil via inductive coupling with the wireless markers.*

Results: Phantom and brain images are shown for the resting, motion-corrected, and motion-corrupted datasets (Fig. 2). Without correction, images are significantly corrupted by motion artifacts (column 3) such as blurring and ghosting. The proposed correction scheme (column 2) results in virtually perfect correction relative to the resting image (column 1), with fine details such as grid-lines (phantom) and vascular structures (brain) being well preserved.

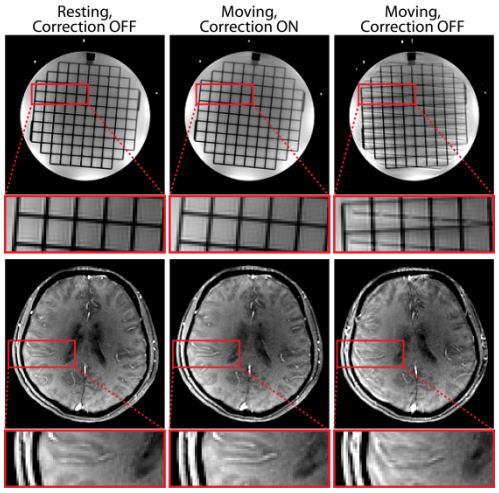

Fig. 2: *Phantom (row 1) and brain images (row 2) acquired without (column 1) and with (column 2, 3) deliberate motion. The phantom experienced a single (~10°) in-plane rotation near the center of k-space. The brain experienced both in-plane (~7°) and through-plane (~2°) rotations throughout the scan. The motions were well reproduced between scans with correction ON (column 2) vs. OFF (column 3). Resting images with correction ON (not shown) were virtually identical to column 1.*

Discussion: A successful prospective correction package using wireless-marker tracking is presented that enables high quality images to be acquired even in the presence of large bulk motions. All electrical cables are eliminated by inductively coupling the wireless markers to the imaging head-coil. Wireless-marker tracking is compatible with intra-image motion compensation, i.e. between single or multiple k-space lines. Because both motion tracking and imaging are performed in the same MR coordinate system, no additional cross-calibration procedure is needed as is the case with optical methods.

The strength of the tracking signal (Fig. 1c) is dependent on the quality of the signal coupling between the wireless markers and imaging head-coil. While signal coupling is dependent on the orientation of the wireless marker relative to the head-coil elements, $\mathbf{B}_0$, and $\mathbf{B}_1$, these issues did not have any practical consequences for the experiments performed here, in which the tracking signal was reliable at all times.

A simple solution to the correspondence problem is implemented that is based on the known relative placement of each wireless marker. More complex solutions, including the use of additional tracking pulse-sequence projections, coil sensitivities, and computer vision algorithms, will be avenues of future research.

Conclusion: Wireless-markers are a good choice to replace wired-markers, as they avoid additional RF-safety risks from electrically conducting wires, and are not hampered by any mechanical connection to the scanner. This provides improved safety/friendliness for patients, together with ease-of-use and minimal setup time for technologists. These advantages may lead the way to more widespread adoption of RF coil based motion tracking in the clinic.

References: [1] Ackerman JL et al., Proc. 5th SMRM 1986;1131-32. [2] Dumoulin CL et al., MRM 1993;29(3):411-15. [3] Derbyshire JA et al., JMRI 1998;8(4):924-32. [4] Krueger S et al., Proc. 14th ISMRM 2006; 3196. [5] Haeberlin M et al., Proc. 20th ISMRM 2012; 595. [6] Ooi MB et al., MRM 2009;62(4):943-54. [7] Ooi MB et al., MRM 2011;66(1):73-81. [8] Ooi MB et al., MRM 2012. [9] Quick HH et al., MRM 2005;53(2):446-455.

Acknowledgements: NIH (2R01 EB00271108-A1, 5RO1 EB008706, 5R01 EB01165402-02), CAMRT at Stanford (P41 EB015891), Lucas Foundation, Oak Foundation. We also thank Paul Calderon, Ralph Hashoian, Mina Makram, Phillip Rossman, Ajit Shankaranarayanan, and Gary Glover.